Supporting Information submitted to JACS

Tuning the size and properties of ClyA nanopores assisted by directed evolution

Misha Soskine, Annemie Biesemans, Marc De Maeyer and Giovanni Maglia

Department of Chemistry, University of Leuven, Leuven, 3001, Belgium

[1]To whom correspondence may be addressed: Email: giovanni.maglia@chem.kuleuven.be

Giovanni Maglia, PhD

Department of Chemistry

University of Leuven

Celestijnenlaan 200G

Heverlee, Leuven Belgium

Tel: +32(0)16 327 696

Email: giovanni.maglia@chem.kuleuven.be

Keywords, single-molecule sensing, folded protein translocation, enhanced stability, permissive oligomerization

Additional results

Selecting cysteine-less variant of ClyA

Since we desired to obtain a cysteine-less ClyA variant amenable to site-specific chemical modification, we subjected ClyA-CS to saturation mutagenesis at position 87 and screened the resulting library. Fixation pattern from previous rounds suggested that clones containing cysteine 87 would show highest activity; therefore, we have isolated and sequenced 12 clones corresponding to medium to high hemolytic activity in the crude lysates. Expectedly, the most active clones contained cysteine at position 87, however, three variants C87A, C87S, C87T with ~10 fold less activity than ClyA-CS did not. ClyA-CS C87A variant, which also displayed an additional mutation H307Y in the His-Tag, was subjected for an additional 5th round of directed evolution. This mutant was chosen because it oligomerized well, formed nanopores that remained open at -150 mV and the codon encoding for the alanine at position 87 could not convert to cysteine via single mutation.

Additional discussion

Electrical Stability of ClyA variants

In planar lipid bilayers two parameters were considered when selecting ClyA variants: low background noise and the absence of gating events. The former could be easily characterized by the power spectrum of a current trace (Figure 4c). The latter could be described as transient or permanent variations in the open pore current (gating), which is most likely due to the spontaneous opening and closing of the nanopore. When the gating event was permanent, flipping the applied potential to

positive and negative values usually restored the open pore current I_O, although for Type III ClyA-CS this was not always possible (Figure S3b). Different batches of proteins showed consistent background noise but inconsistent gating. Typically, below -150 mV Type I ClyA-CS showed less than one gating event per minute while Type II ClyA-CS gated slightly more. Type III ClyA-CS on the other hand could only be used up to ~ -35 mV and even then it often closed to a state of lower conductance that could not be reverted (Figure S3b). Interestingly, at positive applied potentials ClyA was less stable than at negative applied potentials (Figure S3a). Different gating probabilities at opposite applied potentials are often observed with biological nanopores, for example, αHL[1] and MspA[2] nanopores often gate at negative but not at positive applied potentials. Conveniently, however, proteins enter the cis vestibule of ClyA at negative applied potentials[3] and they could thus be sampled up to -150 mV. The factors that influence the entry of analytes into a nanopore are passive diffusion, the applied potential and electroosmosis. By analogy to solid-state nanopores with a negatively charged internal surface,[4] electroosmosis is the most likely dominant force driving HT into ClyA nanopores.[3] This is shown by the fact that proteins despite their charge enter the ClyA pore only at negative applied potentials[3] where the electroosmotic flow from cis to trans is strong (ClyA nanopores are cation selective[5]).

Variation in the dwell time values for HT current blockades

We recurrently observed large variations in HT blockade life times for both Type I and Type II ClyA-CS (Figure S4a). We think this might be due to small differences in the folding of ClyA. Although there are no strong evidences, this interpretation is supported

by the observation that in rare occasions individual ClyA nanopores switched between two substates with slightly different (higher or lower) open pore current (I_O and I_O' inset in Figure S4d) and showing different dwell times for HT induced current blockades (Figure S4d). Crucially, the existence of multiple configurations of the trans-vestibule does not conflict with our interpretation that ClyA might assemble in multiple oligomer states. This is because the differences in the I_O and I_O' (ΔI = 4 pA at -150 mV) are tiny compared to the difference in the open pore currents measured for Type I and Type II ClyA-CS (ΔI = 55 pA at -150 mV, Figure S4d) and the $I_{RES\%}$ values of the current blockades remained largely unaffected (See variation of measured values in Figure S4a versus Figure S4b). In addition, despite the dwell time variations are large, the life times of HT blockades to Type I ClyA-CS were always distinguishable from the life times of HT blockades to Type II ClyA (Figure S4a).

Folded vs unfolded translocation

We assume that while in the vestibule of ClyA, HT is folded under all applied potentials. We base our interpretation on the analysis of the voltage dependence of the residual blocked pore current ($I_{RES\%}$, Figure S4b). When a molecule is lodged within the lumen of a nanopore, the ionic current block is proportional to the atomic volume of the electrolytes being excluded by the molecule.[6-10] Therefore, if the molecule remains folded under different applied voltages, the $I_{RES\%}$ should remain constant. By contrast, if a protein unfolds the $I_{RES\%}$ is expected to change, giving that the length and surface area of the unfolded polypeptide chain is different to that of the globular protein. Therefore, since the residual current of the L2 level of HT blockades remains constant

over the entire potential range considered (Figure S4b) it suggests that HT remains folded while lodged within ClyA-CS.

However, in about 50% of the current blockades to Type I ClyA-CS from -110 to -150 mV, and in less than 10% of the blockades to Type II ClyA-CS nanopores from -90 to -150 mV, the HT current blockades terminated with an additional current level (spike) higher than the open nanopore current (Figure S5). This current spike might be associated to the translocation of the (partially) unfolded HT polypeptide chain through the transmembrane region of ClyA, similar to the transient current increase that is also observed for the translocation of DNA through solid-state nanopores at 150 mM KCl[11] or for the electrophoretic translocation of DNA through carbon nanotubes.[12] This explanation however is not very likely considering the additional ionic current observed in the DNA translocation experiments is most likely due to the counterions associated with the negative charges in DNA,[11] while the charge density of a polypeptide chain is much lower than that of DNA. In addition, the diameter of the trans vestibule of ClyA is relatively large, and protein domains should be able to translocate through ClyA (main text). A more likely explanation is that the α-helices of the transmembrane domain of the ClyA nanopores transiently change conformation allowing the translocation of HT through the pore.

Materials

Unless otherwise specified chemicals were purchased from Sigma-Aldrich, DNA from Integrated DNA Technologies (IDT), enzymes from Fermentas and lipids from

Avanti Polar Lipids. The concentration of human thrombin was calculated from its unit concentrations, assuming that 1 NIH unit/mL = 10 nM. All errors are given as standard deviations. During protein characterization experiments, purified ClyA oligomers were stored at 4°C for several weeks in 0.2% n-Dodecyl-beta-D-Maltoside (DDM) and 5 mM EDTA. Alternatively, we found that ClyA nanopores could be stored for several months at 4°C in excised BN-PAGE gel bands.

Methods

Construction of ClyA libraries by error-prone PCR

Libraries were constructed by amplifying the ClyA genes from plasmid DNA using T7 promoter and T7 terminator primers (Table S2). In the first mutagenesis round we used as a template a plasmid containing the synthetic gene encoding for ClyA-SS from *Salmonella Typhi*(GenScript). From the second mutagenesis round we used the DNA plasmids that were derived from the previous round of selection. In ClyA-SS, the WT sequence was modified by the substitution of the two Cys residues (positions 87 and 285) with Ser and by the attachment of a DNA encoding a Gly-Ser-Ser linker followed by a C-terminal hexahistidine tag.[3]

DNA amplification was performed by error prone PCR: 400 μL of final PCR mix (200 μl of REDTaq ReadyMix, 8 μM final concentration of forward and reverse primers, ~400 ng of plasmid template and ddH_2O up to 400 μl) was split into 8 reaction mixtures containing 0-0.2 mM of $MnCl_2$ and cycled for 27 times (pre-incubation at 95ºC for 3 min, then cycling: denaturation at 95ºC for 15 s, annealing at 55ºC for 15 s, extension at 72ºC for 3 min). These conditions typically yielded 1-4 mutations per gene in the final

library. The PCR products were pooled together, gel purified (QIAquick Gel Extraction Kit, Qiagen) and cloned into a pT7 expression plasmid (pT7-SC1) by MEGAWHOP procedure:[13] ~500 ng of the purified PCR product was mixed with ~300 ng of ClyA-SS circular DNA template and the amplification was carried out with Phire Hot Start II DNA polymerase (Finnzymes) in 50 µL final volume (pre-incubation at 98ºC for 30s, then cycling: denaturation at 98ºC for 5 s, extension at 72ºC for 1.5 min for 30 cycles). The circular template was eliminated by incubation with Dpn I (1 FDU) for 2 hr at 37ºC. The resulted mixture was desalted by dialysis against agarose gel (2.5 % agarose in Milli-Q water) and transformed into *E. cloni*® 10G cells (Lucigen) by electroporation. The transformed bacteria were grown overnight at 37ºC on ampicillin (100 µg/ml) LB agar plates typically resulting in $>10^5$ colonies, and were harvested for library plasmid DNA preparation.

Construction of saturation mutagenesis library at position 87 of evolved ClyA

In order to construct a library containing cysteine–free ClyA variants, the gene encoding for 4ClyA4 (ClyA-CS, Table S1) was amplified using the 87NNS primer (containing a degenerate codon at position 87 encoding for the complete set of amino acids, Table S2) and T7 terminator primers. PCR conditions: 0.3 mL final volume of PCR mix (ReadyMix™), containing ~400 ng of template plasmid, cycled for 30 times (pre-incubation at 95ºC for 3 min, then cycling: denaturation at 95ºC for 15 s, annealing at 55ºC for 15 s, extension at 72ºC for 3 min). The resulting PCR product was cloned

into pT7 expression plasmid by MEGAWHOP procedure using 4ClyA4 circular template (see above).

Construction of the ClyA-WT

ClyA-SS gene was amplified using 87C and 285C primers (Table S2). PCR conditions: 0.3 mL final volume of PCR mix (150 µl of REDTaq ReadyMix, 6µM of forward and reverse primers, ~400 ng of template plasmid), cycled for 27 times (pre-incubation at 95ºC for 3 min, then cycling: denaturation at 95ºC for 15 s, annealing at 55ºC for 15 s, extension at 72ºC for 3 min). The resulting PCR product was cloned into pT7 expression plasmid by the MEGAWHOP procedure described above, using ClyA-SS circular template.

Screening of ClyA libraries and hemolytic assay

Since ClyA-SS displays "border of detection" hemolytic activity, during the first two rounds of the mutagenesis libraries were only screened for activity on Brucella Agar with 5% Horse Blood. From the third selection round, colonies displaying hemolytic activity on Brucella Agar were further screened for hemolytic activity on horse erythrocytes from the crude lysate after overexpression. The goal of this work was to obtain ClyA variants that oligomerised well in DDM and formed nanopores with low electrical noise and uniform unitary conductance in lipid bilayers. Therefore, screening for hemolytic activity alone could not serve as the sole criteria for selection of such variants (for example WT-ClyA is very hemolytically active, but showed non-uniform unitary current distribution). Thus, from the 4th round, proteins from the crude lysate

were purified by Ni-NTA affinity chromatography and the oligomerisation of ClyA was tested on BN-PAGE after incubation in DDM. ClyA nanopores that oligomerised well were then tested in planar lipid bilayers (with particular stress on uniformity of formed channels, low electrical noise and stability at high applied potentials).

Screening for Hemolytic activity on Brucella horse blood agar plates

After the plasmid DNA was electroporated into *E. cloni*® EXPRESS BL21 (DE3) cells (Lucigen), transformants were prescreened on Brucella Agar with 5% Horse Blood (BBL™, Becton, Dickinson and Company) supplemented with 100 µg/ml ampicillin. Clones displaying hemolytic activity, which was observed by a lytic aura around the colonies after overnight growth at 37 ºC, were individually grown in 96-deep-wells plates overnight by shaking at 37ºC (0.5 mL 2xYT medium containing 100µg/mL ampicillin). The obtained cultures were either pooled for preparation of plasmid DNA (QIAprep, Qiagen) that served as a template for the next round (rounds 1 and 2), or used as starters for protein overexpression (rounds 3 to 5).

Screening for hemolytic activity in crude lysates after ClyA overexpression

Rounds 3 to 5: 50 µl of the starter cultures from 400-600 clones (see above) were inoculated into 450 µl of fresh medium in new 96-deep-wells plates and the cultures were grown at 37ºC until OD_{600}~0.8. Then IPTG (0.5 mM) was added to induce overexpression, and the temperature was reduced to 25ºC for an overnight incubation. Next day, bacteria were harvested by centrifugation at 3000 x g for 15 min at 4ºC, the supernatant was discarded and pellets were incubated at -70ºC for few a hours to

facilitate cell disruption. Then pellets were resuspended in 0.3 mL of lysis buffer (15 mM Tris.HCl pH 7.5, 150 mM NaCl, 1 mM $MgCl_2$, 10 µg/ml lysozyme and 0.2 units/mL DNAse I) and lysed by shaking at 1300 RPM for 30 min at 37 ºC. 5-30 µL of lysates were then added to 100 uL of ~1% horse erythrocytes suspension. The latter was prepared by centrifuging horse blood (bioMérieux) at 6000 x g for 5 min at 4 ºC, the pellet was resuspended in 15 mM Tris.HCl pH 7.5, 150 mM NaCl (If the supernatant showed a red color, the solution was centrifuged again and the pellet resuspended in the same buffer). The hemolytic activity was monitored by the decrease in OD at 650nm over time (~3-10 min intervals, measured using Multiskan GO Microplate Spectrophotometer, Thermo Scientific).

Screening for oligomerization and nanopore formation of evolved variants

Rounds 4-5: 6-12 of the most hemolytically active variants were partially purified from the same lysates that were used for the screening of hemolytic activity by using Ni-NTA affinity chromatography: 0.2 mL of crude lysate containing monomeric ClyA was brought to 1 mL with 15 mM Tris.HCl pH 7.5, 150 mM NaCl supplemented with 1% DDM (to trigger ClyA oligomerization) and 10 mM imidazole, incubated at ambient temperature for 20 min and centrifuged at 20,000 x g for 10 min at 4ºC. The clarified lysates were allowed to bind to 20 µL (bead volume) of Ni-NTA agarose beads (Qiagen) for 1 hr by gentle mixing at 4ºC. The unbound fraction was removed by centrifugation at 20,000 x g for 10 min at 4ºC (the supernatant was discarded). Finally, oligomerized ClyA proteins were eluted with 50 µL of 600 mM imidazole in 15 mM Tris.HCl pH 7.5 150 mM NaCl 0.2% DDM. Typically ~40 µg of ClyA was supplemented with ~10% glycerol and 1x of

NativePAGE™ Running Buffer and 1x Cathode Buffer Additive (Invitrogen™) and then loaded on BN-PAGE (Figure S2). Variants that formed oligomers on BN-PAGE were then tested in planar lipid bilayers (with particular stress on uniformity of formed channels).

Protein overexpression and purification

E. cloni® EXPRESS BL21 (DE3) cells were transformed with the pT7 plasmids containing the ClyA gene. Transformants were selected by growth overnight at 37ºC on LB agar plates supplemented with 100 mg/L ampicillin. The resulting colonies were inoculated into LB medium containing 100 mg/L of ampicillin. The culture was grown at 37ºC, with shaking at 200 rpm, until it reached an OD_{600} of 0.6 to 0.8. The expression of ClyA was then induced by the addition of 0.5 mM IPTG and the growth was continued at 20ºC. The next day the bacteria were harvested by centrifugation at 6000 x g for 10 min and the pellets were stored at -70ºC.

The pellets(originated from 50 ml culture) containing monomeric ClyA were thawed and resuspended in 20 mL of wash buffer (10 mM imidazole, 150 mM NaCl, 15 mM Tris.HCl, pH 7.5), supplemented with 1 mM $MgCl_2$ and 0.05 units/mL of DNAse I and the bacteria were lysed by sonication. The crude lysates were clarified by centrifugation at 6000 x g for 20 min and the supernatant was mixed with 200 μL of Ni-NTA resin (Qiagen) in wash buffer. After 1 hr, the resin was loaded into a column (Micro Bio Spin, Bio-Rad) and washed with ~5 ml of the wash buffer. ClyA was eluted with approximately ~0.5 mL of wash buffer containing 300 mM imidazole. Protein concentration was determined by Bradford assay and the purified proteins were stored at 4ºC.

Construction of ClyA models

The 13mer and 14mer ClyA nanopores were modeled from the 12mer of the crystal structure (PDB code: 2WCD) as follow: A central axis was constructed through the length of the 12mer (ax12), and the distance between the C-alpha atom of residue 114 in the monomer A (114Ca-A) and the ax12 was measured giving the approximate radius of the pore (r12). The distance (d) between the 114Ca-A and the equivalent atom in monomer B (114Ca-B) was used to calculate the approximate circumference of the 12mer (c12 = d x 12), 13mer (c13 = d x 13) and 14mer (c14 = d x 14). The radius of the three oligomers (r12, r13 and r14) was then calculated from the circumference using simple trigonometry. The 12mer, 13mer and 14mer were then built by placing the monomers at distances r12, r13 and r14, respectively, from the central ax and rotated over an angle of 360°/12, 360°/13 and 360°/14, respectively. The 12mer that was built using this method reproduced perfectly the 12mer of the X-ray crystal structure (RMS=0.29 Å), showing the high degree of symmetry and feasibility to construct higher order pores.[14]

The size of the nanopore opening was determined by increasing the Van der Waals radii of the atoms of ClyA until the pore closed. Then the increased value of the Van der Waals radii was taken as the radius of the pore. The diameter of thrombin was calculated from a sphere corresponding to the measured molecular volume of the protein.[14]

Electrical recordings in planar lipid bilayers

The applied potential refers to the potential of the trans electrode. ClyA nanopores were inserted into lipid bilayers from the cis compartment, which was connected to the ground. The two compartments were separated by a 25-μm thick polytetrafluoroethylene film (Goodfellow Cambridge Limited) containing an orifice ~100 μm in diameter. The aperture was pretreated with ~5 μL of 10% hexadecane in pentane and a bilayer was formed by the addition of ~10 μL of 1,2-diphytanoyl-*sn*-glycero-3-phosphocholine (DPhPC) in pentane (10 mg/mL) to both electrophysiology chambers. Typically, the addition of 0.01-0.1 ng of oligomeric ClyA to the cis compartment (0.5 mL) was sufficient to obtain a single channel. ClyA nanopores displayed a higher open pore current at positive than at negative applied potentials, which provided a useful tool to determine the orientation of the pore. Electrical recordings were carried out in 150 mM NaCl, 15 mM Tris.HCl pH 7.5. The temperature of the recording chamber was maintained at 28°C by water circulating through a metal case in direct contact with the bottom and sides of the chamber.

Data recording and analysis

Electrical signals from planar bilayer recordings were amplified by using an Axopatch 200B patch clamp amplifier (Axon Instruments) and digitized with a Digidata 1440 A/D converter (Axon Instruments). Data were recorded by using Clampex 10.2 software (Molecular Devices) and the subsequent analysis was carried out with Clampfit software

(Molecular Devices). Open pore currents and HT blockades were recorded by applying a 10 kHz low-pass Bessel filter and sampling at 50 kHz if not otherwise stated. For unitary channel conductance distributions data collection, traces were further filtered digitally with Gaussian low-pass filter with 200 Hz cutoff. The open pore currents were determined for all inserted channels at both +35 and -35 mV to ensure that the pore inserted with the correct orientation and values corresponding to -35 mV were used to construct the distributions. Open pore current values (I_O) for ClyA and blocked pore current values (I_B) for HT were calculated from Gaussian fits to all points histograms (0.3 pA bin size).[3] Histograms for HT blockades were prepared from at least 10 current blockades at least 0.5 s long. The residual current values ($I_{RES\%}$) were calculated as: $I_{RES\%} = I_B / I_O$ %. When HT produced two current levels within the same blockade, their relative contributions (Figure 5a, Table 1) were deduced from the area of the peaks obtained from Gaussian fits to the all points histogram.[3] HT blockade lifetimes were calculated by single exponential fitting of the cumulative distribution of at least 200 current blockades (Figure S7). Graphs were made with Origin (OriginLab Corporation) or Clampfit software (Molecular Devices). All values quoted in this work are based on the average of at least three separate recordings.

Supporting Figures and Tables

Table S1. Mutations accumulated during the directed evolution rounds of the ClyA-SS gene.

Round	Name	Clone ID	Sequence changes relative to ClyA-WT
0	**ClyA-SS**	dSClyA	C87S, C285S
3		3ClyA1	C87S, F166Y, K230R, C285S
3		3ClyA2	Q73R, F166Y, C285S
3		3ClyA3	Q33R, Q56H, C87S, D122G, C285S
4		4ClyA1	I4T, N128S, S145I, C285S
4		4ClyA2	S110I, C285S, F166Y, T223A
4		4ClyA3	T39I, C285S, F166Y, K230R
4	**ClyA-CS**	*4ClyA4*	L99Q, E103G, F166Y, C285S, K294R
4		4ClyA5	I4T, Q73R, C285S
4		4ClyA6	Q73R, F166Y, C285S
5		5ClyA1	C87A, L99Q, E103G, C285S, F166Y, N220S, Q289R, K294R, H307Y
5		5ClyA2	C87A, L99Q, E103G, C285S, F166Y, Q289R, K294R, H307Y
5	**ClyA-AS**	*5ClyA3*	C87A, L99Q, E103G, C285S, F166Y, I203V, K294R, H307Y

Table S2: primers table. N stands for A, G, C, or T; S is G or C, thus NNS codon encodes for the full set of amino acids.

Name	**Sequence**
87NNS	GAAGCTACCCAAACGGTTTACGAATGGNNSGGTGTGGTTACCCAGCTGCTG
T7 promoter	TAATACGACTCACTATAGGG
T7 terminator	GCTAGTTATTGCTCAGCGG
87C	GTTTACGAATGGTGTGGTGTGGTTACCCAG
285C	CGCTGCTGATATTCATTACAGGTATTAATCATTTTC

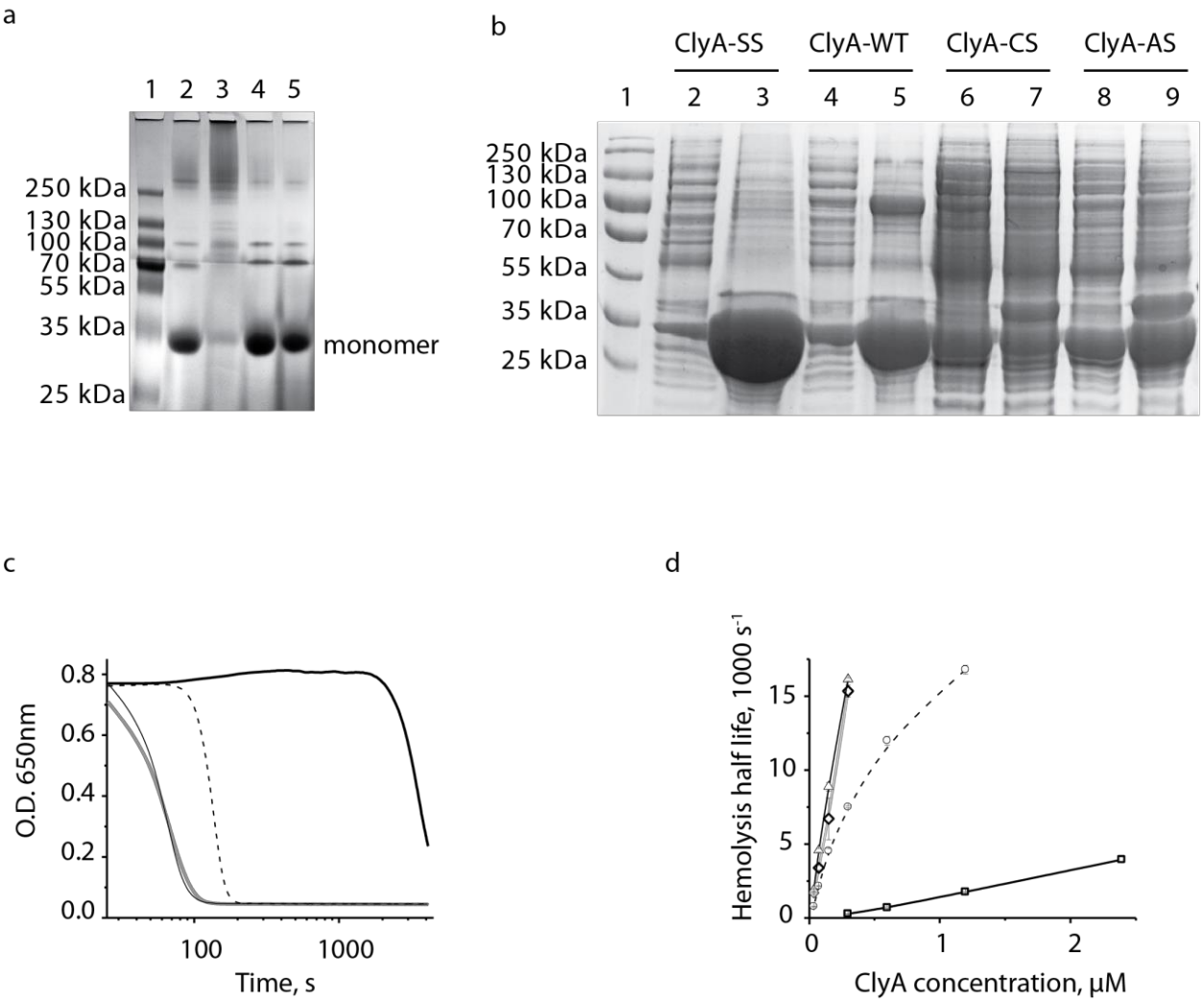

Figure S1. Characterization of purified ClyA monomers. (a) Solubility of purified ClyA monomers examined by 4-20% acrylamide BN-PAGE. Equal amounts (40 µg) of purified ClyA monomers (no detergent) were supplemented with ~10% glycerol and 1x of NativePAGE™ Running Buffer and 1x Cathode Buffer Additive (Invitrogen™) and loaded in each lane: Lane 1: markers, Lane 2: ClyA-WT, Lane 3: ClyA-SS, Lane 4: ClyA-CS, Lane 5: ClyA-AS. (b) Overexpression of ClyA variants. Equal amounts of bacterial pellets derived from overnight cultures overexpressing ClyA variants were resuspended to ~100 mg/mL concentration and disrupted by sonication followed by centrifugation at 20,000g for 10 min (4ºC). 20 µl of the supernatant containing the soluble fraction of ClyA proteins were loaded on lanes 2, 4, 6 and 8 of a 12%

acrylamide SDS-PAGE. The lysate pellets were brought to the original volume by adding a solution containing 15 mM, Tris.HCl pH 7.5, 150 mM NaCl and 2% SDS w/v. 20 μl of such solution were loaded on lanes 3, 5, 7 and 9 of the same 12% acrylamide SDS-PAGE. Therefore, Lane 1: protein marker, Lanes 2 and 3: ClyA-SS supernatant and pellet fractions, respectively; Lanes 4 and 5: ClyA-WT supernatant and pellet fractions, respectively; Lane 6 and 7: ClyA-CS supernatant and pellet fractions, respectively; and Lane 8 and 9: ClyA-AS supernatant and pellet fractions, respectively. (c) Hemolytic assays. ClyA monomers (0.6 μM) were incubated with 100 μl of 1% horse erythrocytes suspension (110 μl final volume) and the decrease of turbidity was measured at 650 nm (OD_{650nm}). ClyA-WT is shown as a thick grey line, ClyA-SS as a thick black line, ClyA-CS as a thin black line and ClyA-AS as a dashed line. d) The rates of hemolysis (calculated as the inverse of the time to reach 50% of turbidity) plotted against protein concentration ClyA-WT (diamonds, thick grey line), ClyA-SS (squares, thick black line), ClyA-AS (circles, dashed line) and ClyA-CS (triangles, thin black line).

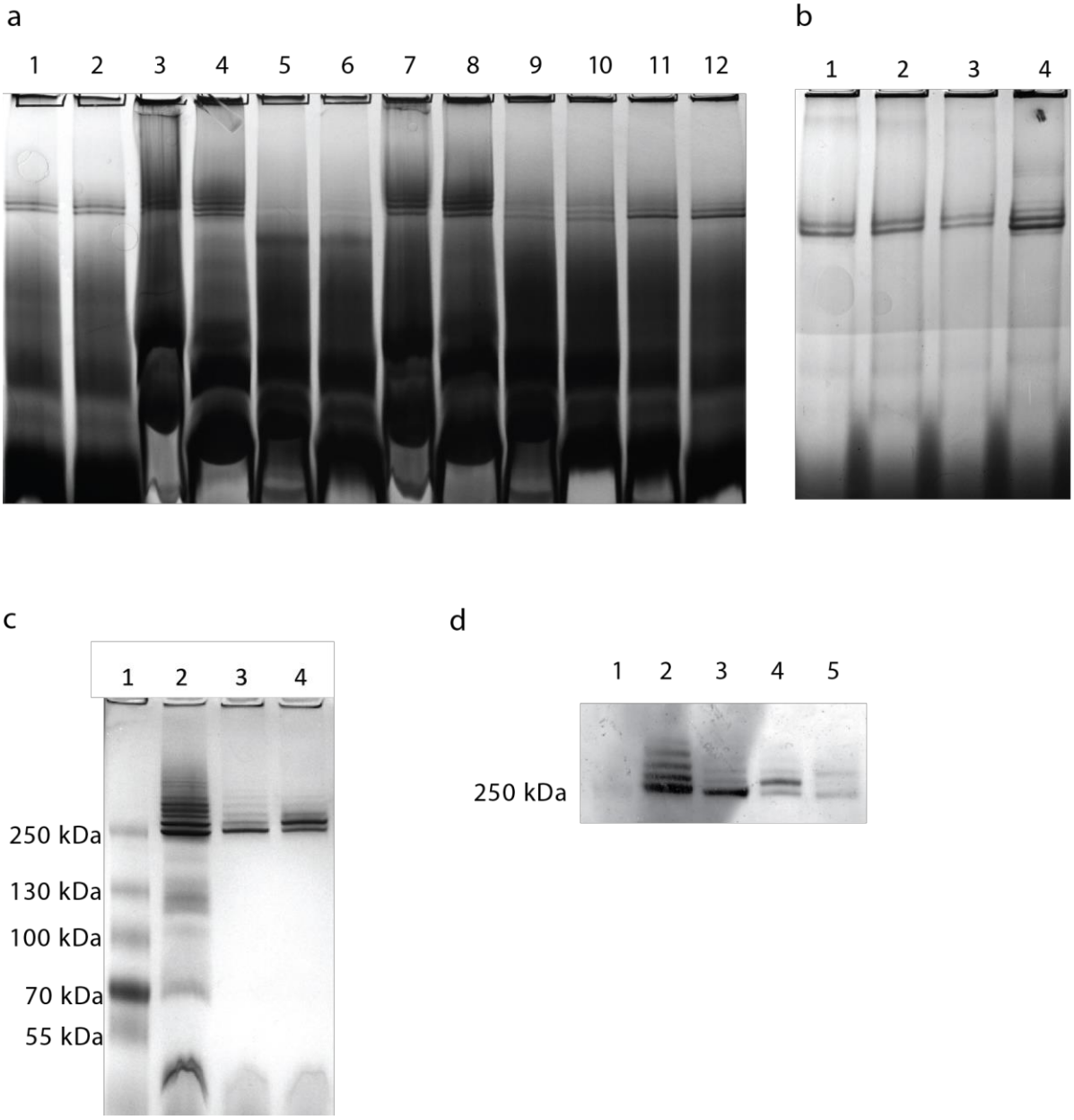

Figure S2. Examples of the screening of ClyA variants oligomerization using 4-20% acrylamide BN-PAGE. (a) Round 4. Lane 1, 2: ClyA-CS, lane 3 and 4: 4ClyA5, lane 5 and 6: 4ClyA3, lane 7 and 8: 4ClyA1, lane 9 and 10: 4ClyA2, lane 11 and 12: 4ClyA6. Samples were prepared as explained in Figure S1a supplemented with 0.05% (even

lane number) or 0.1% (odd lane numbers) SDS. SDS was used to counter the "smearing" effect of large quantity of DDM in the samples. (b) Round 5. Lane 1, 2: 5ClyA2, lane 3: 5ClyA1, lane 4: ClyA-AS. Samples were supplemented with 0.05% SDS. Oligomerization was triggered by the addition of 1% DDM and ClyA variants were partly purified by Ni-NTA affinity chromatography as described in methods. (c) BN-PAGE showing the different ClyA-CS bands extracted from preparative gels developed by Coomassie staining (Figure 2a). Lane 1: Protein ladder, lane 2: ClyA-CS monomers pre-incubated in 0.5% DDM, Lane 3 ClyA-CS pores extracted from the lowest band mainly corresponding to Type I ClyA-CS, lane 4: ClyA-CS pores extracted from the second lowest ClyA band mainly corresponding to Type II ClyA-CS. d) BN-PAGE showing the ClyA-CS bands extracted from preparative (Figure 2a) gels developed by silver staining. Lane 1: Molecular marker, Lane 2: ClyA-CS monomers pre-incubated in 0.5% DDM, Lane 3 ClyA-CS oligomers extracted from the lowest band mainly corresponding to Type I ClyA-CS, lane 4: ClyA-CS oligomers extracted from the second lowest ClyA band mainly corresponding to Type II ClyA-CS. Lane 5: ClyA-CS oligomers extracted from the third lowest ClyA band mainly corresponding to Type III ClyA-CS. ClyA-CS oligomers were extracted in 15 mM Tris.HCl pH 7.5, 150 mM NaCl containing 0.5% DDM and incubated in the same buffer for 30 min prior loading into the gels.

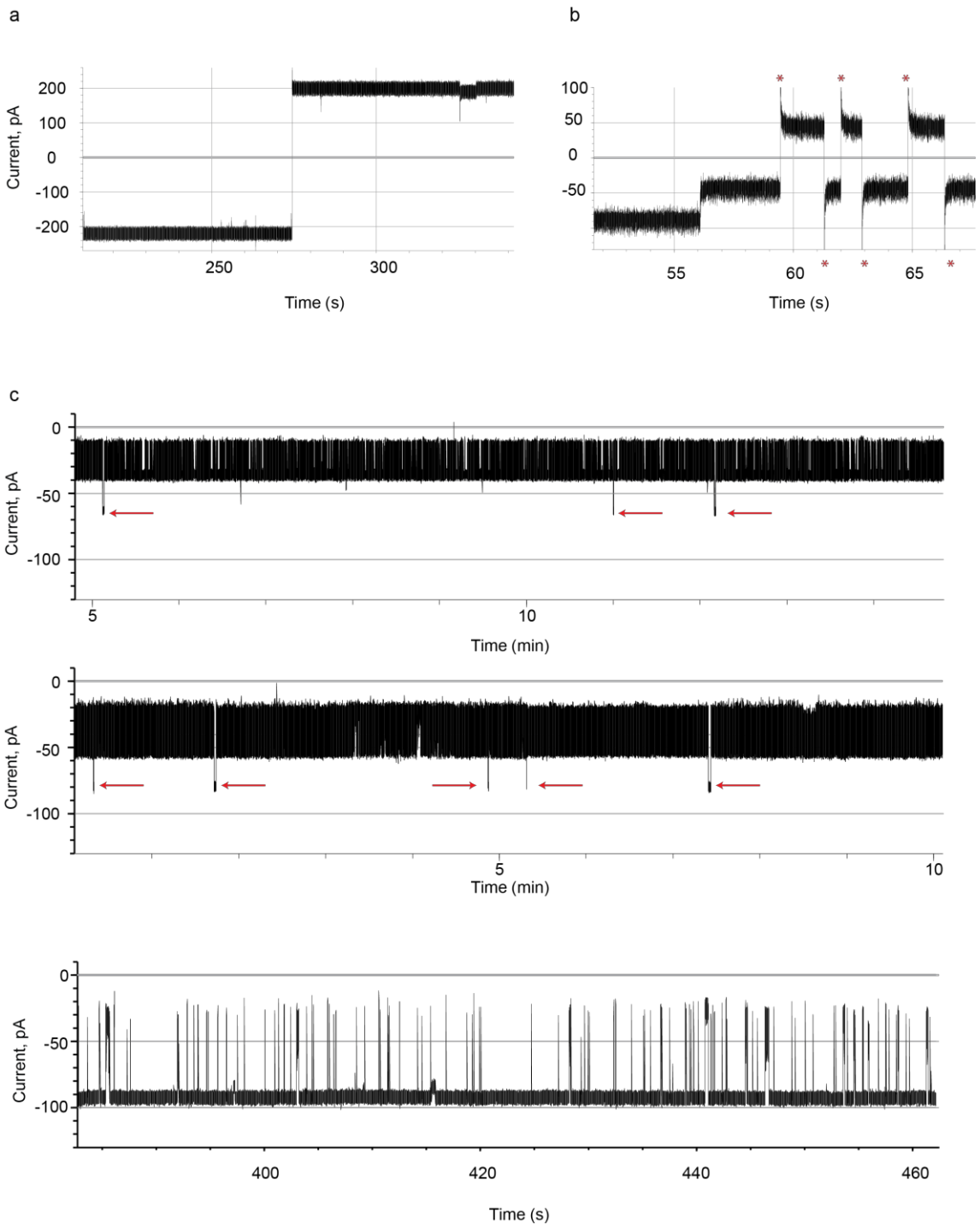

Figure S3. Electrical properties of evolved ClyA-CS nanopores. (a) Current recording of Type I ClyA-CS at -150 mV (left current trace) and after switching the potential to +90 mV (right current trace). (b) Current recording of Type III ClyA-CS showing the permanent closing of the pore at -35 mV. Reversing the potential to positive and negative potentials (red asterisks) did not restore the open pore current. (c) HT current

blockades to Type I (top), Type II (middle) and Type III (bottom) ClyA-CS at -35 mV. Type I and II ClyA-CS open pore currents are shown by a red arrow. The current traces were recorded at a sampling rate of 50 kHz with an internal low-pass Bessel filter set at 10 kHz. For presentation purposes, the current traces were further filtered using a digital Gaussian low-pass filter with a 2 kHz cutoff. Recordings were carried out in 15 mM Tris.HCl, pH 7.5, 150 mM NaCl, 28°C and in presence of 20 nM HT.

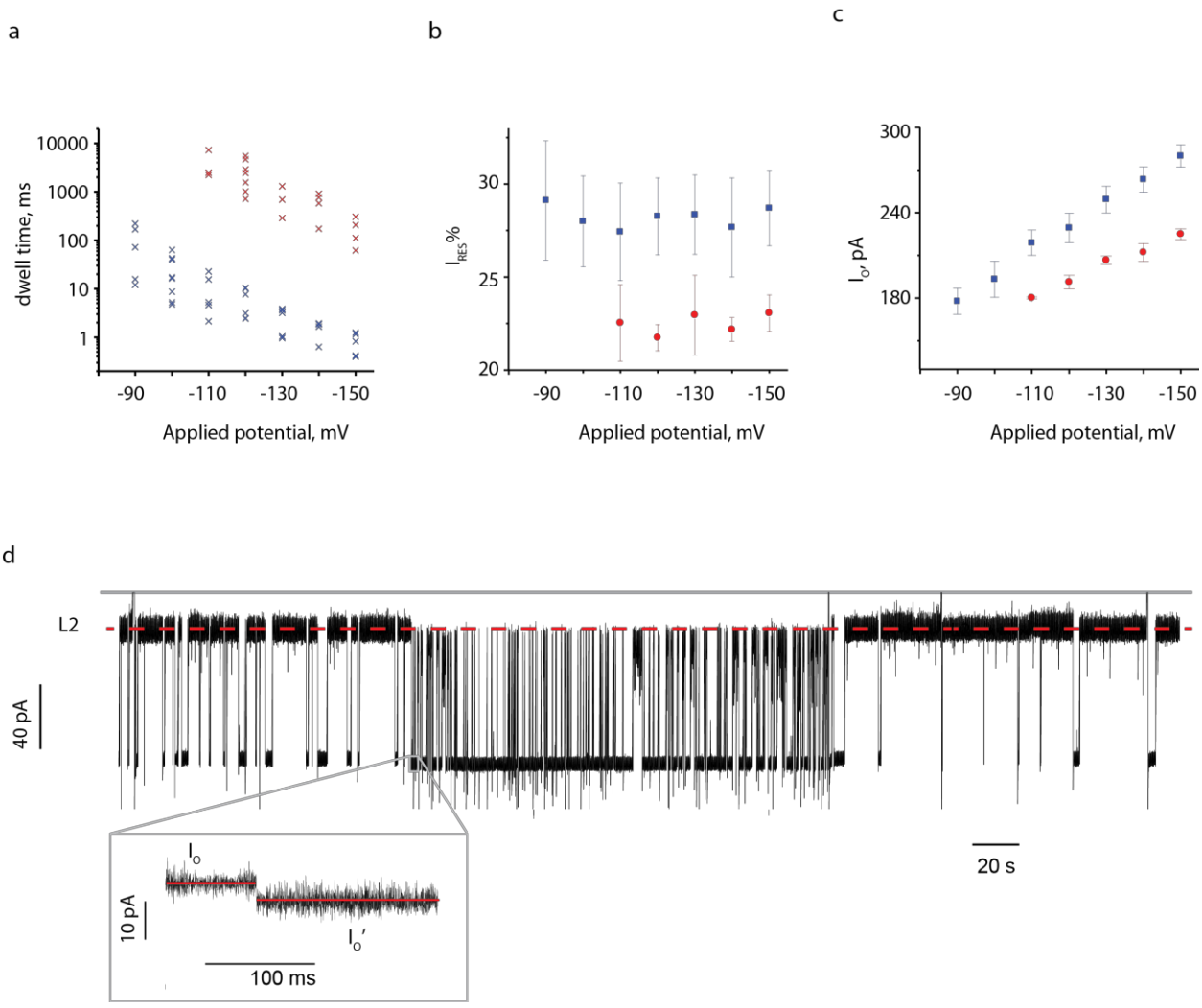

Figure S4. HT current blockades to evolved ClyA-CS nanopores. Voltage dependence of the duration (dwell time, a), residual current ($I_{RES\%}$, b) and open pore current (I_O, c) of HT current blockades to Type I (red) and Type II (blue) ClyA-CS. The large variation of

HT blockade dwell times to both Type I and Type II ClyA (a) might be explained by the existence of ClyA nanopores with different folded states (Additional Discussion). (d) HT current blockades to a Type I ClyA-CS nanopore at -150 mV showing one of the three-recorded cases where a ClyA-CS nanopore transiently switched between two states with different affinity for HT. The inset shows the expanded view where a 4 pA change in the open pore current (from I_O to I_O') defines the transition between the two substates of the pore. Traces were recorded in 15 mM Tris.HCl, pH 7.5, 150 mM NaCl, in presence of 20 nM HT, at a sampling rate of 50 kHz with an internal low-pass Bessel filter set at 10 kHz. Each plotted value corresponds to the average determined using at least 3 different single channels. Errors are given as standard deviations.

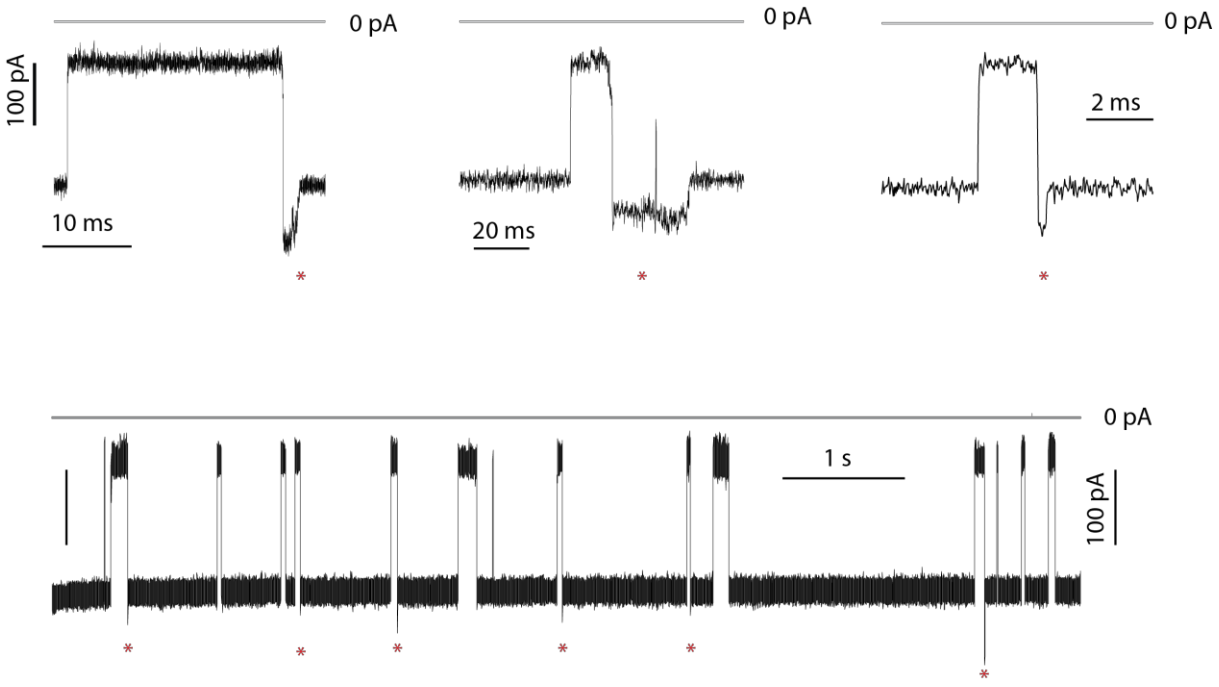

Figure S5. Typical HT current blockades on Type I ClyA-CS at -150 mV showing "spike" current signatures. The red asterisks indicate a current spike. Recordings were carried out in 15 mM Tris.HCl, pH 7.5, 150mM NaCl in presence of 20 nM HT. The traces were filtered with a Gaussian low-pass filter with 10,000 Hz cutoff frequency and sampled at 50,000 Hz.

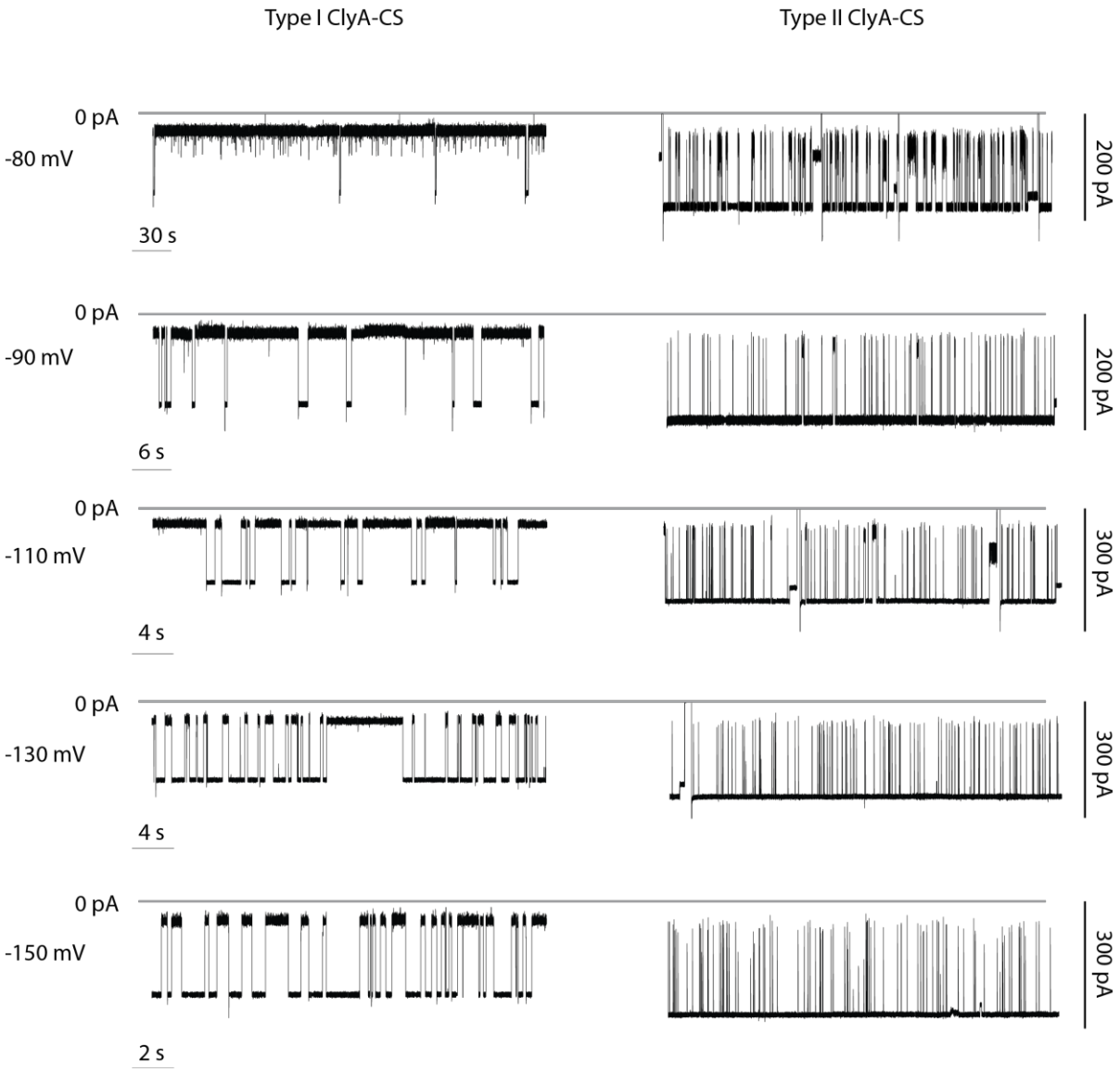

Figure S6. Typical HT current blockades to Type I (left) and Type II (right) ClyA-CS at increasing negative applied potentials (from top to bottom). The current traces were recorded at a sampling rate of 50 kHz with an internal low-pass Bessel filter set at 10 kHz. For presentation purposes, the current traces were further filtered using a digital Gaussian low-pass filter with a 2 kHz cutoff. Recordings were performed in 15 mM Tris.HCl, pH 7.5, 150mM NaCl and 28°C in presence of 10-20 nM HT.

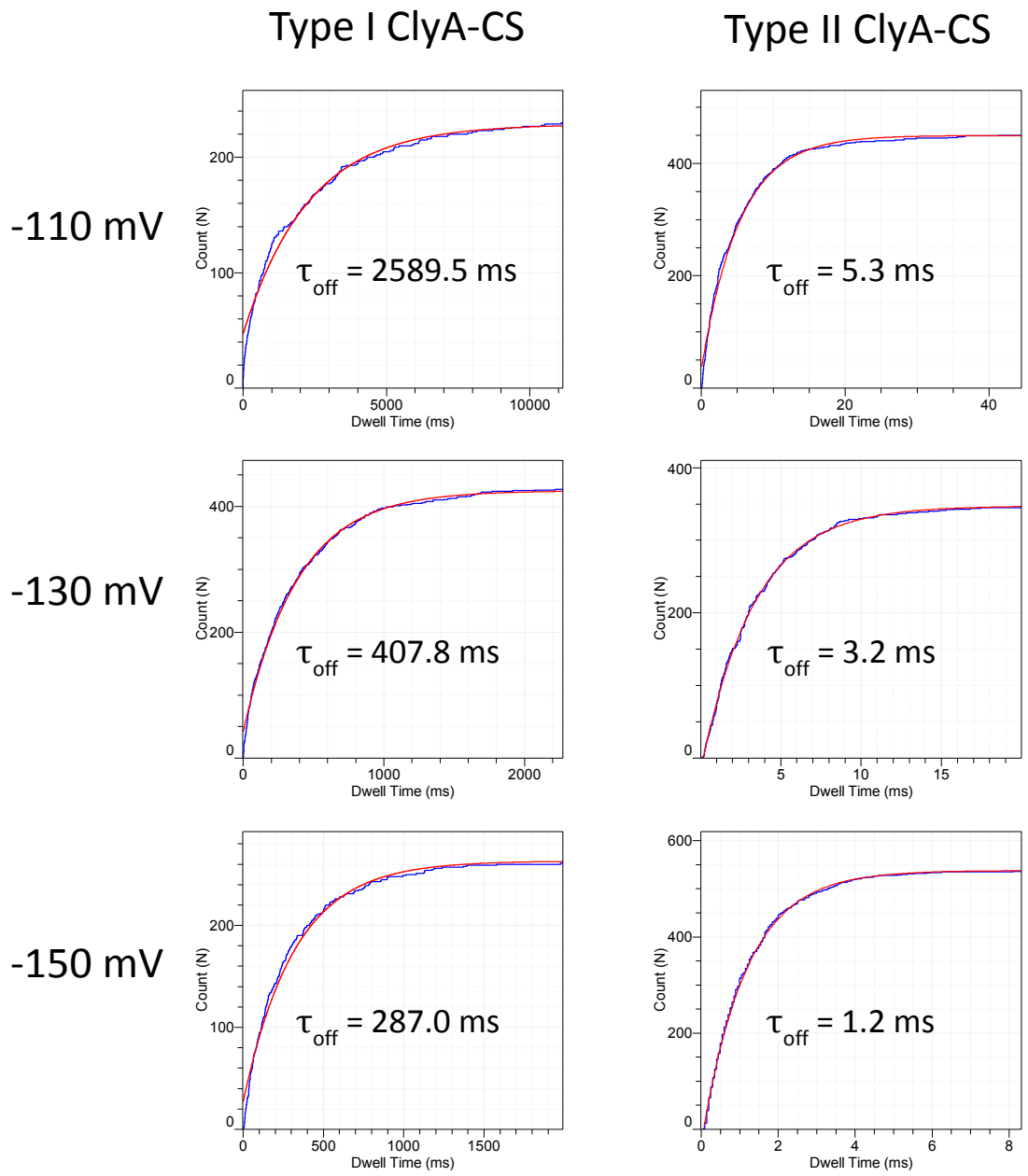

Figure S7. Typical dwell time analysis for HT current blockades to Type I (left) and Type II (right) ClyA-CS at increasing negative applied potentials (from top to bottom). The graphs show single exponential fits (red lines) to cumulative distributions (blue lines) of the collected event lifetimes. Recordings were performed in 15 mM Tris.HCl, pH 7.5, 150mM NaCl and 28°C in presence of 10-20 nM HT.

References

(1) Maglia, G.; Heron, A. J.; Hwang, W. L.; Holden, M. A.; Mikhailova, E.; Li, Q.; Cheley, S.; Bayley, H. *Nat Nanotechnol* **2009**, *4*, 437.

(2) Butler, T. Z.; Pavlenok, M.; Derrington, I. M.; Niederweis, M.; Gundlach, J. H. *Proc Natl Acad Sci U S A* **2008**, *105*, 20647.

(3) Soskine, M.; Biesemans, A.; Moeyaert, B.; Cheley, S.; Bayley, H.; Maglia, G. *Nano Lett* **2012**, *12*, 4895.

(4) Firnkes, M.; Pedone, D.; Knezevic, J.; Doblinger, M.; Rant, U. *Nano Lett* **2010**, *10*, 2162.

(5) Feld, G. K.; Thoren, K. L.; Kintzer, A. F.; Sterling, H. J.; Tang, II; Greenberg, S. G.; Williams, E. R.; Krantz, B. A. *Nat Struct Mol Biol* **2010**, *17*, 1383.

(6) Freedman, K. J.; Jurgens, M.; Prabhu, A.; Ahn, C. W.; Jemth, P.; Edel, J. B.; Kim, M. J. *Anal Chem* **2011**, *83*, 5137.

(7) Niedzwiecki, D. J.; Movileanu, L. *J Vis Exp* **2011**.

(8) Talaga, D. S.; Li, J. *J Am Chem Soc* **2009**, *131*, 9287.

(9) Pavlenok, M.; Derrington, I. M.; Gundlach, J. H.; Niederweis, M. *PLoS One* **2012**, *7*, e38726.

(10) Stefureac, R. I.; Trivedi, D.; Marziali, A.; Lee, J. S. *J Phys Condens Matter* **2010**, *22*, 454133.

(11) Smeets, R. M. M.; Keyser, U. F.; Krapf, D.; Wu, M. Y.; Dekker, N. H.; Dekker, C. *Nano Letters* **2006**, *6*, 89.

(12) Liu, H.; He, J.; Tang, J.; Pang, P.; Cao, D.; Krstic, P.; Joseph, S.; Lindsay, S.; Nuckolls, C. *Science* **2010**, *327*, 64.

(13) Miyazaki, K. *Methods Enzymol* **2011**, *498*, 399.

(14) Delhaise, P.; Bardiaux, M.; Demaeyer, M.; Prevost, M.; Vanbelle, D.; Donneux, J.; Lasters, I.; Vancustem, E.; Alard, P.; Wodak, S. J. *J Mol Graphics* **1988**, *6*, 219.